



Feasibility Study of Using Waste Heat from Gas Pressure Reducing Stations for Water Desalination

Maryam Karami^{1*}, Farima Alikhani²

1. Faculty of Engineering, Kharazmi University, Tehran, Iran

2. Department of Mechanical Engineering, Alzahra University, Tehran, Iran

ARTICLE INFO

ORIGINAL RESEARCH ARTICLE

Article History:

Received: 26 June 2021

Revised: 01 August 2021

Accepted: 21 September 2021

Keywords:

Gas Pressure Reducing Station (PRS)

Water Desalination

Humidification-Dehumidification Unit

Numerical Simulation

Aspen HYSYS

ABSTRACT

In recent years, recovering waste heat to reduce energy consumption and provide the energy needs has become a promising method to solve the energy crisis. In this study, the waste heat from gas pressure reducing stations is used to produce fresh water using a humidification-dehumidification desalination unit. Using Aspen HYSYS to model the proposed system, the effect of different parameters on the fresh water production rate is evaluated. The results show that optimum saline water and air flow rates are 0.165 kg/s and 0.2 kg/s, respectively, for a gas pressure reducing station by a capacity of 50,000 standard cubic meters per hour. It is also found that by decreasing the gas inlet pressure from 1000 psi to 400 psi, the fresh water production rate is decreases by about 52.2%. The increase of the fresh water production rate by increasing the capacity of the pressure reducing station from 10,000 to 50,000 standard cubic meters per hour is about 62%. Furthermore, the fresh production rate at gas pressure reducing station with 10,000 SCM increases 4.4% by increasing the saline water temperature entering the humidifier from 40°C to 80°C.

DOR: [20.1001.1.25885/96.2021.7.2.5.7](https://doi.org/10.25885/96.2021.7.2.5.7)

How to cite this article

M. Karami, F. Alikhani. Feasibility Study of Using Waste Heat from Gas Pressure Reducing Stations for Water Desalination. Journal of Gas Technology. 2021; 6(2): 53 -64. (http://jgt.irangi.org/article_251678.html)

* Corresponding author.

E-mail address: karami@khu.ac.ir (M. Karami)

Available online 26 December 2021

2666-5468/© 2021 The Authors. Published by Iranian Gas Institute.

This is an open access article under the CC BY license. (<https://creativecommons.org/licenses/by/4.0/>)



1. Introduction

Today, the need for drinking water is increasing rapidly. This is while freshwater resources are limited or running low. Only about 3% of the earth's water resources are drinkable. However, 2% of it is frozen in polar glaciers and only 1% of fresh water (FW) is available to humans. On the other hand, the production of FW in the world faced with problems such as significant consumption of fossil fuels or high costs of installation and maintenance of solar collectors. In addition to the excessive costs, it can be also mentioned the production of greenhouse gases and environmental pollution due to fossil fuels. Therefore, it is necessary to use available free energy, which also has low-cost equipment.

There are numerous studies on using waste heat to produce FW (Elsaida et al., 2020; Olabi et al., 2020). Schwantes et al. (2013) performed an experimental investigation on the FW production using a membrane distillation (MD) unit and the waste heat from the cooling circuit of a diesel power station. Their results indicated that the waste heat-based desalination plant operates more steadily than a solar-based desalination unit and the FW of 3688 l is produced in 24 h. Sharshir et al. (2016) designed a combined solar desalination system that includes a humidifier, a dehumidifier and four systems of evaporation and condensation of water vapor. The new desalination system reuses the outlet hot water from humidifier-dehumidifier to supply the secondary system to prevent the loss of hot water during desalination. Reusing the hot drain water increases the system output ratio by 50% and increases the solar still by about 90%. Using the waste heat from gas fired power station for a direct contact membrane distillation (DCMD) system with 0.67 m² of membrane area, Dow et al. (2016) concluded that the FW production is 3 l/(m²h), which depends mostly on the waste heat temperature. Lokare et al. (2017) used the waste heat from natural gas compressor stations for treatment of water generated during

extraction of natural gas from unconventional (shale) reservoirs in Pennsylvania. An ASPEN Plus simulation of DCMD revealed that all the produced water can be treated to 30 wt% regardless of its initial salinity by using the waste heat available from natural gas compressor stations in Pennsylvania.

Lai et al. (2019) recovered the waste heat from the proton exchange membrane fuel cell to produce distilled water using DCMD. They found that the energy utilization degree increases by 201%-266% under maximal energy gain condition. He et al. (2018) proposed a humidification-dehumidification (HDH) system in which seawater is desalinated by heat recovery. The simulation results show that the maximum amount of water production is 99.05 kg/h and the output ratio is 1.51 when the dehumidifier equilibrium conditions appear in the design conditions, while the low cost of water production unit is equal to 37.68 \$/kg.h and the air flow is 0.14 kg/h. Santosh et al. (2018) investigated the performance of a combined HDH system using the waste heat of vapor compression refrigeration (VCR) based on the air conditioning unit. It was found that with increasing air conditioning temperature, the average condensate production decreased. In addition, the economic analysis shows that the cost of FW produced by the proposed system is about \$ 0.1658 per kilogram. Using waste heat from both the exhaust fumes and the cooling water of submarine engines, Shafieian and Khiadani (2020) reported that a DCMD unit can produce 8.3 kg/m²h at cooling water flow rate of 0.25 kg/s and diesel exhaust mass ratio of 0.25.

Sorgulu and Dincer (2021) investigated the performance a hybrid multi-effect desalination (MED) and reverse osmosis (RO) units using biomass-based waste heat. The results show that 92.29 kg/s freshwater is produced using 2.498 kg/s of municipal solid and 0.1314 kg/s of olive oil waste. Shakib et al. (2021) studied using the waste heat from gas turbine cycle for water desalination by hybrid multi-effect thermal vapor compression desalination (MED-TVC)

and reverse osmosis (RO). The FW produced by the proposed system varied between 70,000 m³/day and 140,000 m³/day. The Summary of

previous researches on waste heat-based water desalination is shown in Table 1.

Table 1. Summary of previous researches on waste heat-based water desalination

Author	Desalination unit	Waste heat source	Investigation type	Highlights
Schwantes et al. (2013)	MD	Cooling circuit of a diesel power station	Experimental	<ul style="list-style-type: none"> Waste heat-based desalination plant operates more steadily than a solar-based desalination unit. FW of 3688 l is produced in 24 h.
Sharshir et al. (2016)	HDH and four systems of evaporation and condensation of water vapor	Hot water form HDH	Numerical	<ul style="list-style-type: none"> Daily water production rate is 13 L/h. Reusing the hot drain water increases the system output ratio by 50%. It also increases the solar still by about 90%.
Dow et al. (2016)	DCMD	Gas fired power station	Experimental	<ul style="list-style-type: none"> FW production rate is 3 l/(m²h), which depends mostly on the waste heat temperature.
Lokare et al. (2017)	DCMD	Natural gas compressor stations	Numerical	<ul style="list-style-type: none"> All produced water can be treated to 30 wt% regardless of its initial salinity.
Lai et al. (2019)	DCMD	Proton exchange membrane fuel cell	Numerical	<ul style="list-style-type: none"> FW mass flow rate can lead to the maximal energy gain. Energy utilization degree increases by 201%-266% under maximal energy gain condition
He et al. (2018)	HDH	Exhaust gas	Numerical	<ul style="list-style-type: none"> Maximum amount of water production is 99.05 kg/h. Output ratio is 1.51 at the dehumidifier equilibrium conditions. Low cost of water production unit is 37.68 \$/kg.h.
Santosh et al. (2018)	Hybrid HDH-VCR	Vapor compression refrigeration (VCR)	Numerical and Experimental	<ul style="list-style-type: none"> By increasing air conditioning temperature, the average condensate production decreased. Cost of FW produced is about \$ 0.1658 per kilogram. Maximum average freshwater yield is 4.63 kg/h and 4.13 kg/h.
Shafieian and Khiadani (2020)	DCMC	Exhaust fumes and cooling water of submarine engines	Numerical	<ul style="list-style-type: none"> Freshwater productivity is more sensitive to temperature than mass flow rate. FW of 8.3 kg/m²h produces at cooling water flow rate of 0.25 kg/s and diesel exhaust mass ratio of 0.25
Sorgulu and Dincer (2021)	Hybrid MED-RO	Biomass	Numerical	<ul style="list-style-type: none"> Overall energy and exergy efficiencies are 37.04% and 19.78%, respectively 92.29 kg/s freshwater is produced using 2.498 kg/s of municipal solid and 0.1314 kg/s of olive oil waste.
Shakib et al. (2021)	Hybrid MED-TVC/RO	Gas turbine cycle	Numerical	<ul style="list-style-type: none"> FW production rate varied between 70,000m³/day and 140,000 m³/day. Lowest production cost is obtained using the cooling water of MED-TVC as the RO system feed water.

Natural gas pressure reducing stations at the inlets of suburban gas networks are responsible for regulating and reducing gas pressure. This pressure drop is from the range of 1000-1200 psi to about 250 psi. The pressure reduction process that occurs by the regulator reduces the temperature due to the positive Joule-Thomson coefficient. This decrease in temperature is so great that it causes the gas to freeze and condense. To prevent this problem, the gas is heated in the water bath heater before reaching the regulator. Most part of the fuel energy used in the heater is always wasted by exhausting the combustion products. Some attempts have been made to use this waste heat for various applications. Ghaebi et al. (2018) investigated using the waste heat of PRS heater for produce power and hydrogen. They combined a Rankine cycle (RC), an absorption power cycle (APC), and a proton exchange membrane (PEM) electrolyzer. The results indicate that the thermal and exergy efficiency of the combined PRS/PEM-RC systems were 32.9% and 47.9%, respectively, while these values for combined PRS/APC system were 33.6% and 48.9%, respectively. Naderi et al. (2018a) studied the performance of a water reheating system installed on the chimney of the heater. They found that the fuel consumption of the heater reduces by about 45% and the payback period is about 1.3 years. In another study, they reported that the heat exchanger with the coolant flow of 1.3 kg/s and fin per inch of 3.3 has the minimum pressure drop (Naderi et al., 2018b). By using the waste heat of the PRS heater for preheating the water inside the heater, Karami and Noroozi (2019) concluded that the energy consumption of heaters is decreased by about 50% and also, the heater efficiency increases by 20%.

One way to reuse this waste heat is desalinating of salt water to meet the needs of people for FW, which is one of the important issues and crises ahead. In an interesting work, Deymi-Dashtebayaz et al. (2021) proposed a multi-effect desalination thermal vapor compression (MED-TVC) system to produce FW using the waste heat of PRS heater. Their analysis showed that the optimal station

capacity for a two effect MED-TVC system is a PRS with capacity of 11.5 kg/s.

As the literature review shows, there is no study on recovering the waste heat of a PRS heater for producing the FW with a small-scale HDH unit. Therefore, in this study, the thermal performance of a humidification-dehumidification desalination unit is investigated using the waste heat from the water bath heater of a PRS. The effect of the operating parameters on the FW production rate is evaluated by simulating the proposed system in Aspen HYSYS.

2. System description and simulation

The schematic of the proposed PRS-HDH system is indicated in Figure 1. The natural gas flow is heated passing the bath water heater to the desired temperature (usually 30 °C) and then, is throttled by the regulator to the desired pressure, which is normally 250 psi. The combustion products, which are still the high temperature heat source, flows in the heater chimney and goes to a heat exchanger, in which transfers its heat to the saline water flow from the dehumidifier. Then, the warm saline water is sprayed into the humidifier and is vaporized and absorbed by the air. This humid air goes to the dehumidifier and can be distilled and recycled by passing from cold surfaces to produce distilled water. The governing mass and energy conservation equations on the performance of the PRS heater and the HDH unit are defined in the following sections.

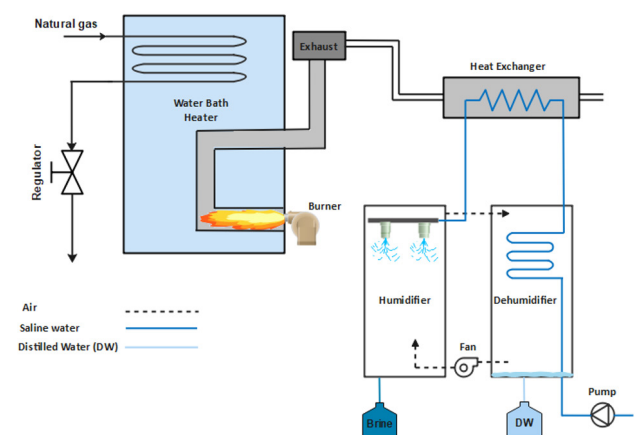


Figure 1. Schematic of the proposed PRS-HDH system

2.1. PRS heater

In water bath heaters, the combustion products outlet from the burner cause the water temperature inside the heater to rise and the water heats indirectly the natural gas inside the tubes. The schematic of the heater is shown in Figure 1. Therefore, considering the water bath heater as a control volume, the law of energy conservation is as follows (Bayat et al., 2016):

$$\dot{Q}_{load} = \dot{Q}_{swf} + \dot{Q}_{NG} + \dot{Q}_{water} \quad (1)$$

where \dot{Q}_{load} is the heating value of the fuel, \dot{Q}_{NG} is the heat transfer rate received by the natural gas, \dot{Q}_{water} is the required heat transfer rate for increasing the water temperature inside the heater, and \dot{Q}_{shl} is the heat loss due to radiation and convection from the heater surface.

The thermodynamics first law is used to calculate \dot{Q}_{NG} as following:

$$\dot{Q}_{NG} = \dot{m}_{NG} (h_{out} - h_{in}) = \dot{m}_{NG} \int_{T_i}^{T_{ou}} c_{p,NG} dT \quad (2)$$

where \dot{m}_{NG} is the mass flow rate of natural gas and $C_{p,NG}$ is its specific heat, which is obtained as a function of temperature from the following relation:

$$c_{p,mix} = \sum X_i \times c_{p,i} \quad (3)$$

where X_i is the mass fraction of the natural gas component and $C_{p,i}$ is their specific heats. The combustion process has the constant pressure and all components are considered as ideal gas.

To determine \dot{Q}_{shl} , the temperature of the heater inside surface is considered equal to the temperature of the hot water inside heater:

$$\dot{Q}_{shl} = \frac{T_w - T_{am}}{\sum R_t} \quad (4)$$

where T_w is the temperature of heater inside water and R_t is the total thermal resistance of heater wall.

The required heat transfer rate for increasing the water temperature inside the heater (\dot{Q}_{water}) is calculated as follows:

$$\dot{Q}_{water} = \int_i^{i+l} \dot{m}_w \cdot c_{p,w} dT \quad (5)$$

The period of the calculation is one hour:

The heat transfer rate of the heater is calculated using \dot{Q}_{load} and \dot{Q}_{losses} :

$$\dot{Q}_{heater} = \frac{\dot{Q}_{load}}{\eta_c} + \dot{Q}_{losses} \quad (6)$$

where η_c is the heater efficiency:

The volumetric flow rate of the fuel is obtained using the following relation:

$$\dot{V} = \frac{\dot{Q}_{heater}}{LHV} \quad (7)$$

2.2. HDH desalination unit

In Figure 2, the schematic of a closed air open water (CAOW) HDH desalination unit and its component is shown. The mass and energy conservation equations and the heat exchanger relations are used to model the performance of the HDH unit. It is assumed that the air flow is steady state and fully developed with constant thermo-physical properties. Considering the dehumidifier as a control volume, the mass, and energy conservation equations are written as follows (Narayan et al., 2010):

$$\dot{m}_{pw} = \dot{m}_a (\omega_{a,2} - \omega_{a,1}) \quad (8)$$

$$\dot{m}_w (h_{w,1} - h_{w,0}) + \dot{m}_{pw} h_{pw} = \dot{m}_a (h_{a,2} - h_{a,1}) \quad (9)$$

The mass and energy conservation equations for the humidifier are written as follows (Narayan et al., 2010):

$$\dot{m}_w - \dot{m}_a (\omega_{a,2} - \omega_{1,a}) = \dot{m}_b \quad (10)$$

$$\dot{m}_a (h_{a,1} - h_{a,2}) = \dot{m}_b h_{w,3} - \dot{m}_w h_{w,2} \quad (11)$$

The heat transfer from the collector to the fluid is obtained by using the following equation:

$$\dot{Q}_{heater} = \dot{m}_w c_{p,w} (T_{w,2} - T_{w,1}) \quad (12)$$

The gained output ratio (GOR) of the HDH is defined as:

$$GOR = \frac{\dot{m}_{fw} \cdot h_{fg}}{\dot{Q}_{in}} \quad (13)$$

where \dot{m}_{fw} , h_{fg} and \dot{Q}_{in} are fresh water mass flow rate, evaporation enthalpy and inlet thermal energy to the HDH

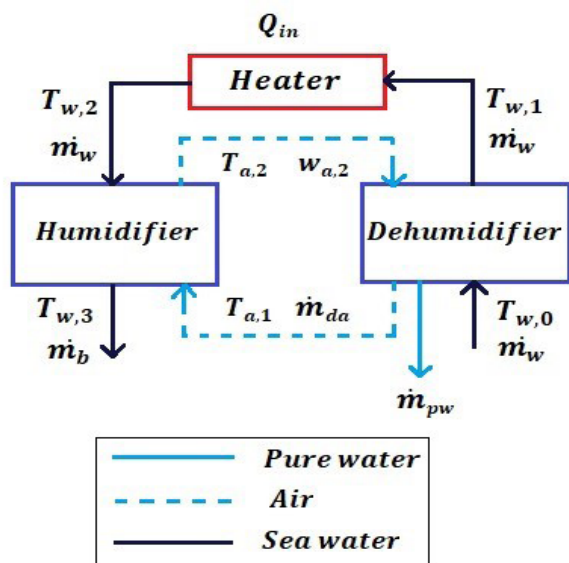


Figure 2. Schematic of a CAOW-HDH desalination system

2.3. Validation

Since there is no experimental data to validate the integrated PRS-HDH system, the PRS and HDH models are separately validated using the experimental results.

For validating the PRS model, the calculated gas outlet temperature from the model is compared with the gas outlet temperature from the PRS of Semnan

(Rastgar and Saedodin, 2013), which have measured in 10 days. The PRS characteristics are entered to the HYSYS model. Figure 3 indicates that the model has the proper accuracy and the mean absolute percentage error (MAPE) is 5.5%.

2.4. Simulation

Figure 5 indicates the HYSYS model of the proposed PRS-HDH system. The features and HYSYS types of the components used to simulate

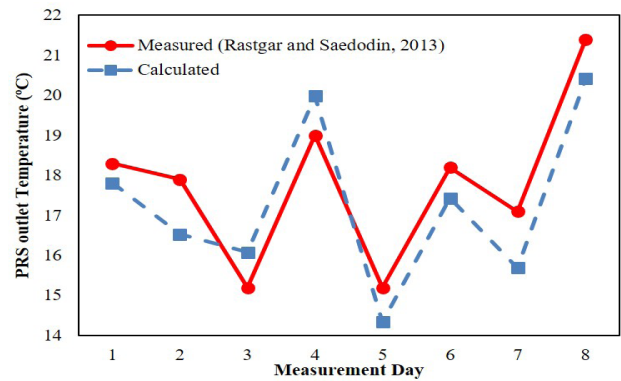


Figure 3. Comparison of measured (Rastgar and Saedodin, 2013) and calculated PRS outlet temperature

The results of the HDH model are compared with the results of the experimental study (Narayan et al., 2010). Table 2 indicates the measured and calculated GOR of the HDH in different saline water inlet temperature. As can be seen in Table 2, the experimental and numerical results were in good agreement by the MAPE of 6.2%.

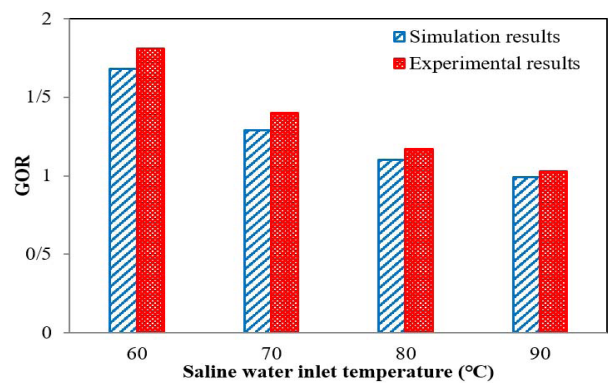


Figure 4. Comparison of the experimental (Narayan et al., 2010) and numerical GOR

the system are listed in Table 2. The specifications of the natural gas in the simulated PRS are shown in Table 3. To illuminate the simulation process, a flowchart is shown in Figure 6.

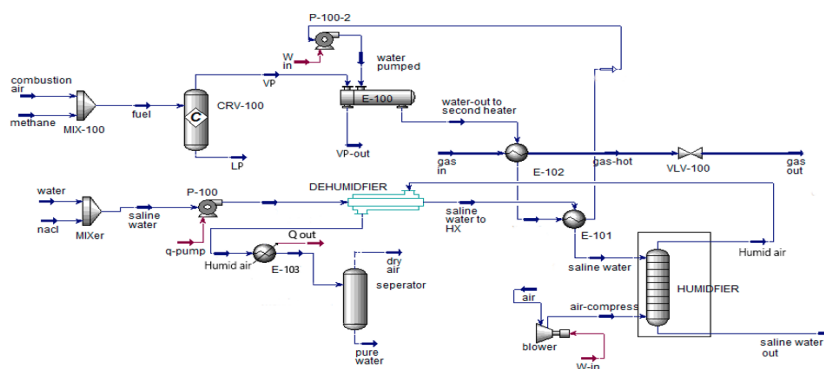


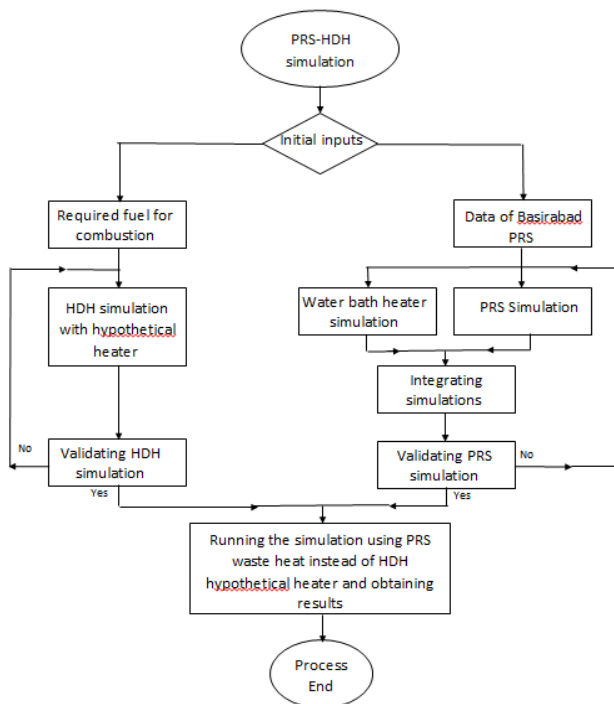
Figure 5. Simulation of the PRS-HDH system in Aspen HYSYS

Table 2. Features and HYSY type of the main components used in the simulation

Component	Features
Regulator	Type: VLV-100 Temperature [°C]: 30 Pressure [psia]: 994 Volume flow rate [m ³ /h]: 50,000
Pump	Type: P-100 Power [kW]: 0.02 Mass flow rate [kg/s]: 1.44 Pressure difference [psia]: 15.23
Reactor	Type: CRV-100 Reaction set: $CH_4 + 2O_2 \rightarrow CO_2 + 2H_2O$ Volume flow rate [m ³ /h]: 771.4 Product temperature [°C]: 1835
Shell and tube heat exchanger	Type: E-100 VP temperature [°C]: 1835 VP outlet temperature [°C]: 69 Pumped water temperature [°C]: 66.95 Water-outlet to second heater temperature [°C]: 158
	Type: E-101 Water inlet temperature [°C]: 69.85 Water outlet temperature [°C]: 66.94 Saline water to HX temperature [°C]: 50 Saline water to humidifier temperature [°C]: 66
	Type: E-102 Inlet gas temperature [°C]: 10 Outlet gas temperature [°C]: 30 Water inlet to second heater temperature [°C]: 158 Water outlet temperature [°C]: 69.85
Mixer	Mixing water with salt to produce a seawater fluid with mole fraction below: H ₂ O: 0.9873 NaCl: 0.0127 Mass flow rate [kg/s]: 0.28
Separator	Separating H ₂ O from humid air with phase fractions below: Moisture air [H ₂ O-air]: 0.0774- 0.9225 Pure water Mass Flow [kg/s]: 0.03 Dry air Mass Flow[kg/s]: 0.66
Dehumidifier	Type: Shell and tube Saline water-pumped temperature [°C]: 25.01 Saline water to HX temperature [°C]: 50 Humid air temperature [°C]: 54.92 Humid air to cooler temperature [°C]: 45.07
Humidifier	Type: Absorber Add H ₂ O to dry air with phase fractions below: Humid air[H ₂ O-Air]: 0.0625- 0.9375

Table 3 Analysis of natural gas

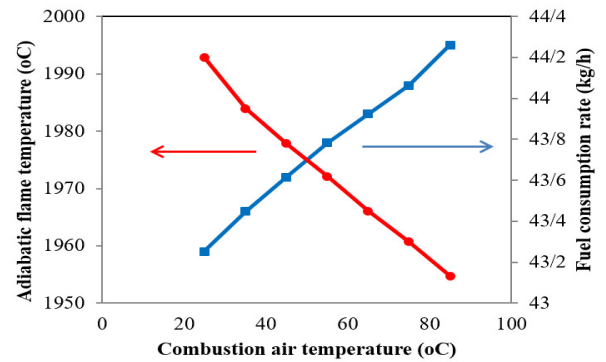
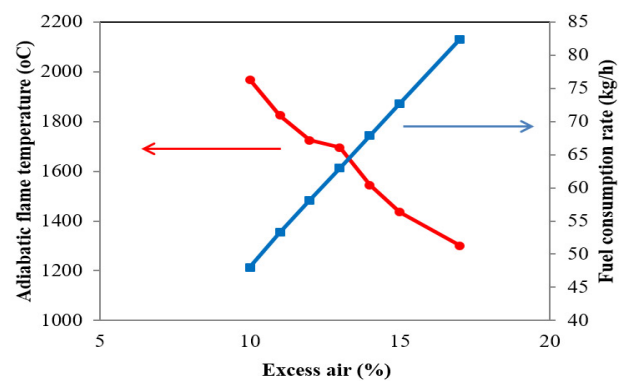
Components	Mole fraction (%)
CH ₄	95.4
N ₂	0.9
CO ₂	0.1
C ₂ H ₆	2.3
C ₃ H ₈	0.75
ISO - C ₄ H ₁₀	0.13
N - C ₄ H ₁₀	0.2
ISO - C ₅ H ₁₂	0.08
N - C ₅ H ₁₂	0.08
C ₆ H ₁₄	0.04
C ₇ H ₁₆	0.02

**Figure 6. Flowchart of simulation process**

3. Results and discussion

Figure 7 indicates the effect of combustion air temperature and excess air percentage on the adiabatic flame temperature and fuel consumption of the PRS burner. By increasing the temperature of air entering the burner, the combustion efficiency increases and the adiabatic flame temperature and thus, the fuel consumption reduces, as can be seen in Figure 7 (a). According to Figure 7 (b), increasing the

percentage of excess air reduces the adiabatic flame temperature and thus, reduces the heat transfer from the combustion gases to the fire tube and more fuel is used to compensate for this shortcoming.

**(a)****(b)****Figure 7. Variation of adiabatic flame temperature and fuel consumption by (a) combustion air temperature and (b) excess air**

The variation of FW production rate by the mass flow rate of saline water and air are depicted in Figure 8. By increasing the mass flow rate of saline water to a desirable point, it is obvious that the production of the FW increases. However, after saturating the air by the water vapor, increasing the saline water flow rate has negative effect on the FW production rate, because the air temperature increases and then, the dehumidification process deteriorated. By increasing the air flow rate, the capacity of the air for absorbing more water vapor increases and therefore, the more FW is produced. However, similar to the saline water flow rate, the FW production rate decreases by increasing the air flow rate beyond the optimum value of the air

flow rate. This is because the water flow rate is constant and therefore, the released heat from the dehumidification process heats up less the air entering the humidifier. The results show that optimum saline water and air flow rate are 0.165 kg/s and 0.2 kg/s, respectively. In other words, the ratio of saline water to air flow rates should be 0.825 to produce the highest FW by the proposed system.

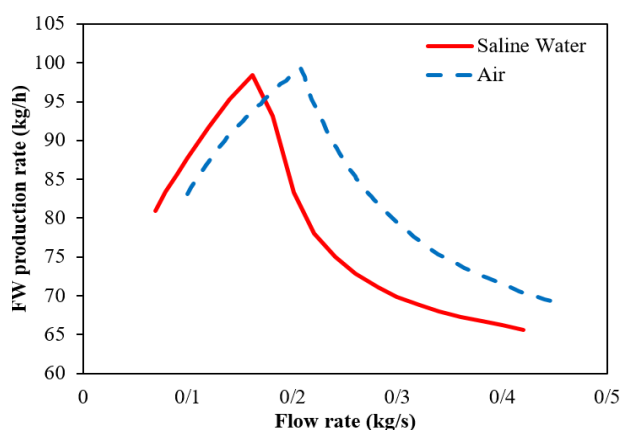


Figure 8. Variation of FW production rate by saline water and air mass flow rate

The variation of the FW production by the gas inlet pressure is indicated in Figure 9. By decreasing the gas inlet pressure, the fuel is required to heat the gas to the desired temperature in the heater reduces and therefore, the lower thermal energy delivers to the saline water and the FW production rate decreases. By decreasing the gas inlet pressure from 1000 psi to 400 psi, the FW production rate is decreases by about 52.2%.

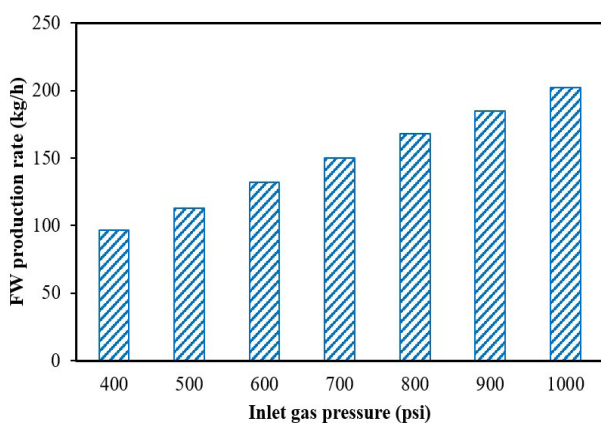


Figure 9. Effect of gas inlet pressure on FW production rate

In Figure 10, the effect of gas flow rate of the PRSs in four different cities of Iran on the FW production rate is indicated. The PRS capacities are listed in Table 4. As observed, the FW production rate increases by increasing the gas flow rate because of the higher thermal energy of the combustion products which are used for heating the saline water entering the humidifier. The increase of the FW production rate by increasing the PRS capacity from 10,000 to 50,000 standard cubic meters per hour (SCMH) is about 62%.

Table 4 Capacity of different PRSs

Station name	Basirabad	Arjan	Bistoon	Shahrood
Station capacity (SCMH)	50,000	30,000	20,000	10,000

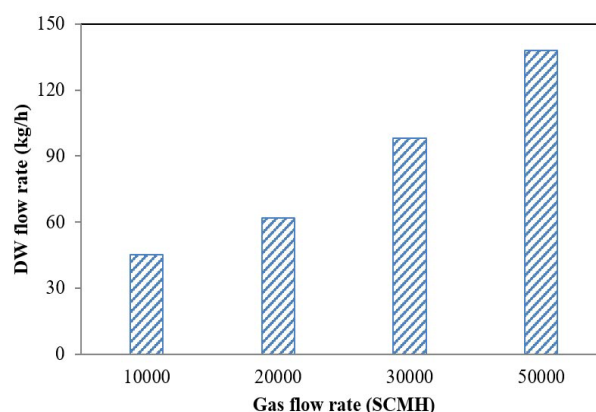
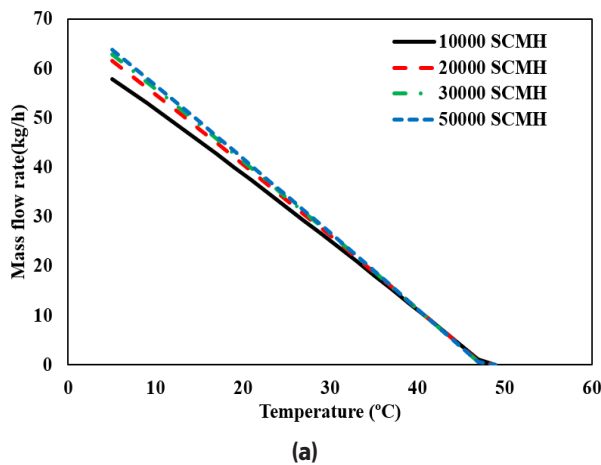


Figure 10. Effect of gas flow rate on FW production rate

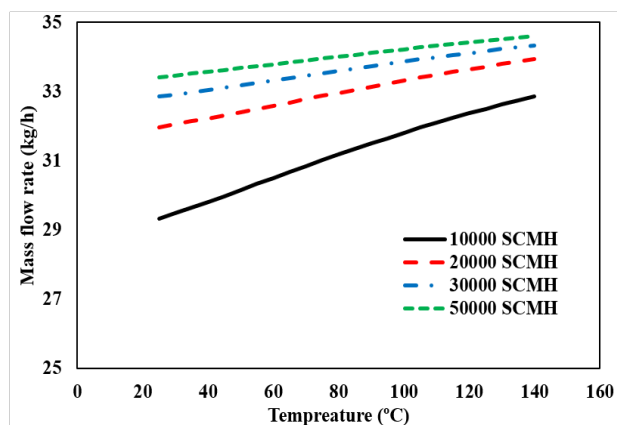
The effect of the temperature of spray water into the humidifier and the temperature of saline water into the dehumidifier on the DW production rate is depicted in Figure 11. As can be seen, by increasing the capacity of the PRS, the FW production increases because of more heat transfer rate from the combustion products to the saline water. In Figure 7 (a), it is shown that the higher the temperature of the inlet water to the dehumidifier, the lower the heat exchange and the lower the capacity of the water to absorb heat from the air, and as a result, the air cools less and the water vapor in it becomes less condensed. By increasing the saline water temperature from 10°C to 40°C, the fresh production rate at PRS

with 10,000 SCMh decreases about 73.4%. This value for PRS with 50,000 SCMh is about 73.7%.

According to Figure 11 (b), the higher the temperature of the spray water in the humidifier, the more moisture the air absorbs and the FW production increases. Furthermore, it is found that by increasing the spray water temperature from 40°C to 80°C, the fresh production rate at PRS with 10,000 SCMh increases 4.4%. It should be noted that if the saline water temperature is too low, the spray water temperature reduces, which has an adverse effect on FW production; therefore, there is a limit for saline water temperature.



(a)



(b)

Figure 11 Effect of temperature of inlet saline water to (a) dehumidifier and (b) humidifier on FW production rate

4. Conclusions

In this study, the thermal performance of the PRS-HDH system integrating PRS heater

with HDH desalination unit has been studied. It should be noted that a fixed HDH size is assumed for all PRSs because the fresh water production of the PRSs can be compared. Also, the heat exchangers, humidifier, and dehumidifier are considered insulated. Furthermore, it is assumed that the complete combustion process is occurred in a constant pressure chamber. The findings showed that by increasing the temperature of the combustion air, the combustion efficiency increases and the adiabatic flame temperature and thus, the fuel consumption reduces. Whereas, increasing the excess air percentage reduces the adiabatic flame temperature and thus, fuel consumption increases. It is also found that the production rate of the FW increases by increasing the mass flow rate of saline water, until the air is saturated with water vapor. Then, the production of FW decreases. The higher temperature of the inlet saline water to the dehumidifier results in the lower FW production rate. This is because the less heat exchange between the air and saline water and the lower the capacity of the water to absorb heat from the air. The higher spray water temperature in the humidifier results in the larger FW production rate because of more moisture absorbs by the air. Based on the obtained results, by increasing the air flow rate, the capacity of the air for absorbing more water vapor increases and therefore, the more FW is produced. However, the FW production rate decreases by increasing the air flow rate beyond the optimum value, because the released heat from the dehumidification process heats up less the inlet air to the humidifier. The results show that the ratio of saline water to air flow rates should be 0.825 to produce the highest FW by the proposed system. Considering the operating parameters of the PRS indicated that by decreasing the gas inlet pressure from 1000 psi to 400 psi, the FW production rate is decreases by about 52.2%. Furthermore, the increase of the FW production rate by increasing the PRS capacity from 10,000 SCMh to 50,000 SCMh is about 62%.

Nomenclature

c_p	Specific heat, kJ/kg K
h	Specific enthalpy, J/kg
\dot{m}	Mass flow rate (kg/s)
\dot{Q}	Heat transfer rate(KJ/h)
R	Thermal resistance, K/W
T	Temperature, K
X	Mass fraction

Greek Symbols

η	Efficiency
ω	Absolute humidity, kg_w/kg_{da}

Subscripts

a	air
am	Ambient
i	Component
in	Inlet
out	Outlet
pw	Product water
max	Maximum
mix	Mixture
t	Thermal
w	Water

Abbreviation

LHV	Low heating value
NG	Natural gas
SWF	Surface heat loss
LP	Liquid product
VLV	Valve
VP	Vapor product

Acknowledgements

The authors would like to express their thank to Kharazmi University for the financial supports (under a grant presented by Vice Chancellor in Research).

References

- Bayat, A., Abbasporsani, K., Heidari, F., Vosough, M., 2016. Thermodynamic analysis of gas preheater at Zanjan city gate station, Applied mechanics research 8(1), 27-32.
- Deymi-Dashtebayaz, M., Dadpour, D., Khadem, J., 2021. Using the potential of energy losses in gas pressure reduction stations for producing power and FW. Desalination 497, 114763.
- Dow, N., Gray, S., Li, J., Zhang, J., Ostarcevic, E., 2016. A. Liubinas, P. Atherton, G. Roeszler, A. Gibbs, M. Duke, Pilot trial of membrane distillation driven by low grade waste heat: Membrane fouling and energy assessment. Desalination 391, 30–42.
- Elsaida, K., Taha Sayed, E., Yousef, B.A.A., Rabaia, M.K.H., Abdelkareem, M.A., Olabi, A.G., 2020. Recent progress on the utilization of waste heat for desalination: A review. Energy Conversion and Management 221, 113105.
- Ghaebi, H., Farhang, B., Rostamzadeh, H., Parikhani, T., 2018. Energy, exergy, economic and environmental (4E) analysis of using city gate station (PRS) heater waste for power and hydrogen production: A comparative study. International Journal of Hydrogen Energy 43, 1855-1874.
- He, W., Han, D., Zhu, W.P., Ji, C., 2018. Thermo-economic analysis of a water-heated humidification-dehumidification desalination system with waste heat recovery. Energy Conversion and Management 160, 182-190.
- Karami, M., Noroozi, A., 2019. Application of Waste Heat Recovery Unit for PRS Heater, Journal of Gas Technology 4 (1), 16-23.
- Lai, X., Long, R., Liu, Z., Liu, W., 2018. A hybrid system using direct contact membrane distillation for water production to harvest waste heat from the proton exchange membrane fuel cell. Energy 147, 578-586.
- Lokare, O.R., Tavakkoli, S., Rodriguez, G., Khanna,

- V. Vidic, R.D., 2017. Integrating membrane distillation with waste heat from natural gas compressor stations for produced water treatment in Pennsylvania. *Desalination* 413, 144-53.
- Naderi, M., Ahmadi, G., Zarringhalam, M., Akbari, O., Khalili, E., 2018a. Application of water reheating system for waste heat recovery in NG pressure reduction stations, with experimental verification. *Energy* 162, 1183-1192.
- Naderi, M., Zargar, G., Khalili, E., 2018b. A Numerical Study on Using Air Cooler Heat Exchanger for Low Grade Energy Recovery from Exhaust Flue Gas in Natural Gas Pressure Reduction Stations, *Iranian Journal of Oil & Gas Science and Technology* 7 (1), 93-109.
- Narayan, G.P., Sharqawy, M.H., Lienhard, V., Zubair, S.M., 2010. Thermodynamic analysis of humidification dehumidification desalination cycles. *Desalin. Water Treat.* 16 (1-3), 339-353.
- Olabi, A.G., Elsaid, K., Rabaia, M.K.H., Askalany, A.A., Abdelkareem, M.A., 2020. Waste heat-driven desalination systems: Perspectiv. *Energy* 209, 118373.
- Rastgar, S., Saedodin, S., 2013. Presenting a thermodynamic model to prevent the formation of gaseous hydrates in Natural gas pressure reducing station, 2nd National Iranian Conference on Gas Hydrate, Semnan, Iran.
- Santosh, R., Kumaresan, G., Selvaraj, S., Arunkumar, T., Velraj, R., 2019. Investigation of humidification-dehumidification desalination system through waste heat recovery from household air conditioning unit. *Desalination* 467, 1-11.
- Schwantes, R., Cipollina, A., Gross, F., Koschikowski, J., Pfeifle, D., Rolletschek, M., Subiel, V., 2013. Membrane distillation: Solar and waste heat driven demonstration plants for desalination. *Desalination* 323, 93-106.
- Shafieian, A., Khiadan, M., 2020. A multipurpose desalination, cooling, and air-conditioning system powered by waste heat recovery from diesel exhaust fumes and cooling water. *Case Studies in Thermal Engineering* 21, 100702.
- Shakib, S.E., Amidpour, M., Boghrati, M., Ghafurian, M.M., Esmaili, A., 2021. New approaches to low production cost and low emissions through hybrid MED-TVC+RO desalination system coupled to a gas turbine cycle. *Journal of Cleaner Production* 295, 126402.
- Sharshir, S., Peng, G., Yang, N., El-Samadony, M.O.A., Kabeel, A.E., 2016. A continuous desalination system using humidification-dehumidification and a solar still with an evacuated solar water heater. *Applied Thermal Engineering* 104, 734-742.
- Sorgulu, F., Dincer, I., 2021. Development and assessment of a biomass-based cogeneration system with desalination. *Applied Thermal Engineering* 185, 116432.

امکان سنجی استفاده از گرمای اتلافی ایستگاه کاهش فشار گاز برای شیرین سازی آب

• مریم کرمی^{۱*}، فریما علیخانی^۲

۱. گروه مهندسی مکانیک، دانشکده فنی مهندسی، دانشگاه خوارزمی، تهران، ایران

۲. گروه مهندسی مکانیک، دانشگاه الزهراء، تهران، ایران

(ایمیل نویسنده مسئول: karami@khu.ac.ir)

چکیده

در سال‌های اخیر، بازیابی گرمای اتلافی برای کاهش مصرف انرژی و تأمین انرژی موردنیاز به یک روش امیدبخش برای حل بحران انرژی تبدیل شده است. در این مطالعه، از گرمای اتلافی ایستگاه‌های کاهش فشار گاز برای تولید آب شیرین با استفاده از یک واحد آب‌شیرین‌کن رطوبت زنی - رطوبت‌زدایی استفاده شده است. با مدل‌سازی سیستم پیشنهادی در نرم‌افزار اسپن هایسیس، تأثیر پارامترهای مختلف بر میزان تولید آب شیرین ارزیابی شده است. نتایج نشان می‌دهد که میزان بهینه دبی آب‌شور و جریان هوا برای یک ایستگاه کاهش فشار گاز با ظرفیت ۵۰,۰۰۰ مترمکعب استاندارد بر ساعت (SCMH)، به ترتیب ۰/۱۶۵ کیلوگرم بر ثانیه و ۰/۲ کیلوگرم بر ثانیه است. همچنین مشخص شده است که با کاهش فشار ورودی گاز از ۱۰۰۰ psi به ۴۰۰ psi، میزان تولید آب شیرین حدود ۵۲/۲٪ کاهش می‌یابد. افزایش نرخ تولید آب شیرین با افزایش ظرفیت ایستگاه کاهش فشار از ۱۰,۰۰۰ SCMH به ۵۰,۰۰۰ FG TG حدود ۶۲٪ است. علاوه بر این، میزان تولید آب شیرین در ایستگاه کاهش فشار گاز با ۱۰,۰۰۰ SCMH با افزایش دمای آب‌شور ورودی به رطوبت زن از ۴۰°C به ۸۰°C حدود ۴/۴٪ افزایش می‌یابد.

واژگان کلیدی: ایستگاه کاهش فشار گاز، شیرین سازی آب، واحد رطوبت زنی-رطوبت‌زدایی، شبیه سازی عددی، اسپن هایسیس